*Int. J. Electrochem. Sci.*, 4 **(2009)** 1770 - 1778

**International Journal of ELECTROCHEMICAL SCIENCE**
www.electrochemsci.org

# Improved High Rate Cycling of Li-rich $Li_{1.10}Ni_{1/3}Co_{1/3}Mn_{1/3}O_2$ Cathode for Lithium Batteries

*R. Santhanam, B. Rambabu*[*]

Solid State Ionics and Surface Sciences Lab, Department of Physics, Southern University and A&M College, Baton Rouge, LA 70813, USA
[*]E-mail: rambabu@cox.net

*Received:* 15 October 2009 / *Accepted:* 1 December 2009 / *Published:* 31 December 2009

Layered Li-rich $Li_{1.10}Ni_{1/3}Co_{1/3}Mn_{1/3}O_2$ materials was synthesized and characterized as cathode material for high rate lithium batteries. Li-rich $Li_{1.10}Ni_{1/3}Co_{1/3}Mn_{1/3}O_2$ material show much better capacity retention at high C-rate than stoichiometric $LiNi_{1/3}Co_{1/3}Mn_{1/3}O_2$ in the voltage range between 2.5Vand 4.3V. Li-rich cathode material shows the discharge capacity of 123 mAh/g with capacity retention of 91% when compared to 80% for the stoichiometric cathode material, in 30 cycles at a high C-rate of 8C. The improved cycling behavior and higher reversible capacity of the Li-rich $Li_{1.10}Ni_{1/3}Co_{1/3}Mn_{1/3}O_2$ material compared to the stoichiometric $LiNi_{1/3}Co_{1/3}Mn_{1/3}O_2$ could probably be due to an improved structural stability by the formation of $Li_2MnO_3$ like domains by the excess lithium ions reside in the transition metal layer.

**Keywords:** lithium metal oxide, sol-gel method, high rate, lithium batteries

## 1. INTRODUCTION

Lithium ion batteries with high energy density and power density are used to power notebook computers, cellular phones, and digital cameras and more recently hybrid electric vehicles (HEVs), plug-in hybrid electric vehicles (PHEVs) and full electric vehicles (FEVs) [1-3]. $LiCoO_2$ is the primary cathode material in commercial lithium ion battery because it is reasonably easy to synthesize and has excellent electrochemical properties [4, 5]. However, the cost of Co, toxicity and structural deterioration when more than 0.5 Li is removed from $LiCoO_2$ have prevented more widespread use of the $LiCoO_2$ cathode material in lithium ion batteries. Because of those limitations, and safety concerns, there is a strong interest in developing alternative, low cost cathode materials. In this regard, materials based on mixed Ni, Mn and Co have been proposed as the alternative positive electrode materials to replace $LiCoO_2$. Ohzuku and Makimura initially proposed novel materials namely $LiNi_{0.5}Mn_{0.5}O_2$ and

$LiNi_{1/3}Co_{1/3}Mn_{1/3}O_2$ as promising cathode materials for lithium rechargeable batteries [6, 7]. Recently, intensive work has been carried out towards development of these materials as possible replacement for $LiCoO_2$ in lithium ion batteries [8-15]. Among those materials, $LiNi_{1/3}Co_{1/3}Mn_{1/3}O_2$ has been studied extensively as promising cathode material for lithium ion batteries. Electronic structure studies have shown that it consists of $Ni^{2+}$, $Mn^{4+}$ and $Co^{3+}$, and reversible capacity involves the oxidation of $Ni^{2+}$ to $Ni^{4+}$ with a two-electron transfer during the initial stage of $Co^{3+}$ to $Co^{4+}$ in the later stage [16-20]. Thus the higher capacity of layered $LiNi_{1/3}Co_{1/3}Mn_{1/3}O_2$ could be due to the improved chemical stability associated $Ni^{2+/3+}$ and the $Ni^{3+/4+}$ redox couple compared to $Co^{3+/4+}$ redox couple.

The electrochemical performance of various lithium metal oxides has been reported to depend on many experimental parameters such synthesis methods, nature of raw materials, sintering temperature, and surface modifications [21-25]. However, Li-rich $LiNi_{1/3}Co_{1/3}Mn_{1/3}O_2$ is of particular interest because unlike $LiNiO_2$ or $LiCoO_2$, $LiNi_{1/3}Co_{1/3}Mn_{1/3}O_2$ can accommodate considerable amount of lithium in the transition metal sites without altering the overall structure of the material. This is due to the fact that the oxidation state of nickel is +2 in the material whereas the Ni and Co ions in $LiNiO_2$ and $LiCoO_2$ have the nominal oxidation state of +3. In order to accept excess lithium ions in the transition metal site the metal ion in the lithium metal oxide has to be oxidized. It is known that the oxidation of $Ni^{3+}$ / $Co^{3+}$ to $Ni^{4+}$ / $Co^{4+}$ under normal experimental conditions is difficult whereas the oxidation of $Ni^{2+}$ to $Ni^{3+}$ is relatively easier to accept excess lithium in the transition metal sites. Thackeray et al suggested that the lithium-rich compounds with layered structure show quite interesting electrochemical properties to the electrode materials by improving structural stability by the formation of two component composite material like $xLi_2MnO_3$. $(1-x)LiMO_2$ [26]. In this work, stoichiometric and Li-rich $LiNi_{1/3}Co_{1/3}Mn_{1/3}O_2$ cathode materials have been prepared by sol-gel method and the effects of excess lithium on the capacity, rate capability and cycleability at high C-rate are reported.

## 2. EXPERIMENTAL PART

Li-rich $Li_{1.10}Ni_{1/3}Co_{1/3}Mn_{1/3}O_2$ powders were prepared by citric acid-assisted sol-gel process [27]. A required amount of lithium acetate [$Li(CH_3COO)\cdot 2H_2O$], nickel acetate [$Ni(CH_3COO)_2\cdot 4H_2O$], cobalt acetate [$Co(CH_3COO)_2\cdot 4H_2O$], and manganese acetate [$Mn(CH_3COO)_2\cdot 4H_2O$], were dissolved in an appropriate quantity of distilled water at room temperature. The solution was stirred at 50°C and the citric acid was added to the solution which acts as chelating agent in the polymeric matrix. The pH of the solution was adjusted to 7.0 by slowly dropping ammonium hydroxide drop wise and continued stirring for 4 h. The temperature of the solution was raised to 80–90°C and continued stirring till the solution turned into high-viscous gel. The resulted gel was dried at 100°C for 24 h in a temperature controlled oven of an accuracy of ±1°C. The $Li_{1.10}Ni_{1/3}Co_{1/3}Mn_{1/3}O_2$ precursor powder was ground to fine powder and sintered at 450°C under oxygen flowing conditions with a constant heating followed by cooling rate at 4 ◦Cmin−1 to decompose organic constituents. The sintered powder was ground to a fine powder and re-sintered successively at 850°C for 12 h and heating and cooling rate was maintained at 2°Cmin−1 and the

accuracy of the furnace temperature is ±5°C. The preparation procedure is illustrated schematically in scheme 1. For comparison, stoichiometric $LiNi_{1/3}Co_{1/3}Mn_{1/3}O_2$was also prepared by the sol-gel process as described above.

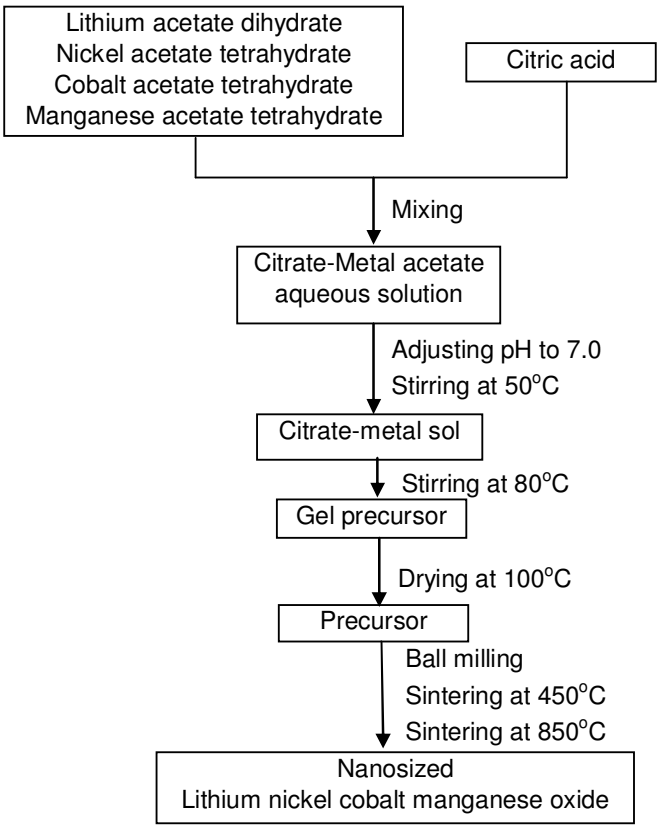


**Scheme 1.** Schematic representation of the synthesis of the nanosized lithium nickel cobalt manganese oxide by citric acid assisted sol-gel process

The Li, Co, Ni and Mn contents in the resulting materials were analyzed using an inductively coupled plasma/atomic emission spectrometer (ICP/AES). The measured composition of the materials is close to the target composition so that the nominal compositions are used to describe the materials throughout this paper for simplicity. The phase purity was verified from powder X-ray diffraction (XRD) measurements. The particle morphology of the powders after sintering was obtained using a scanning electron microscopy (SEM). Electrochemical characterization was carried out with a coin-type cell. The synthesized $Li_{1.10}Ni_{1/3}Co_{1/3}Mn_{1/3}O_2$ cathode was prepared by mixing an 85:10:05 (w/w) ratio of active materials, carbon black, and polyvinylidene fluoride binder, respectively, in N-methyl pyrrolidinone. The resulting paste was cast on an aluminum current collector. The entire assembly was dried under vacuum overnight and then heated in an oven at 120 ◦C for 2 h. The coin cell was made using $Li_{1.10}Ni_{1/3}Co_{1/3}Mn_{1/3}O_2$ as a cathode, lithium metal foil as an anode and 1.0M $LiPF_6$ as in ethylene carbonate (EC) : diethyl carbonate (DEC) (1:1) solvent used as an electrolyte. The polypropylene separator was soaked in an electrolyte for 24 h prior to use. The entire coin cell

assembly was carried out in an argon-filled glove box in which both the moisture and oxygen contents were maintained at less than 2 ppm. The charge and discharge measurements were carried out at different C-rates over the potential range of 2.5–4.3V using Arbin battery tester at room temperature. The electrochemical data were duplicated to ensure reproducibility.

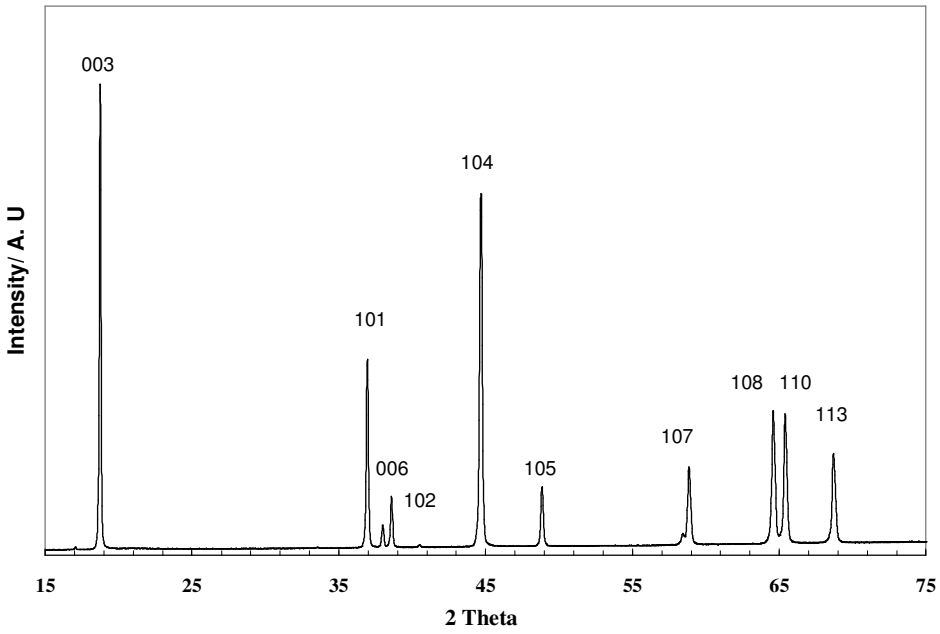


**Figure 1.** XRD patterns of $Li_{1.10}Ni_{1/3}Co_{1/3}Mn_{1/3}O_2$

## 3. RESULTS AND DISCUSSION

X-Ray diffraction technique was employed to evaluate the crystal structure of the synthesized materials obtained by citric acid assisted sol-gel process. The XRD patterns of the nanosized $Li_{1.10}Ni_{1/3}Co_{1/3}Mn_{1/3}O_2$ is presented in Fig.1. All the diffraction peaks can be indexed as a layered oxide structure based on a hexagonal α-$NaFeO_2$ structure (space group R3m). No impurities and secondary phases are observed in this figure. The structure has Li ions at the 3a, the transition metal ions (M= Co, Ni, Mn) at 3b and O ions at 6c sites. Since the ionic radii of $Ni^{2+}$ (0.69 Å) and $Li^+$ (0.76 Å) is similar, a partial interchange of occupancy of Li and nickel ions among the sites (i.e. Li in 3b and Ni in 3a sites) are expected (cation mixing) and that would give rise to disordering in the structure [24]. It has been suggested that cation mixing is known to deteriorate the electrochemical performance of the above-layered compounds. The integrated intensity ratio of the (0 0 3) to (1 0 4) lines (R) in the XRD patterns was shown to be a measurement of the cation mixing and a value of $R < 1.2$ is an indication of undesirable cation mixing [28]. The oxygen sublattice in the -$NaFeO_2$ type structure is considered as distorted from the fcc array in the direction of hexagonal c-axis [29,30]. This distortion

gives rise to a splitting of the lines assigned to the Miller indices (0 0 6, 1 0 2) and (1 0 8, 1 1 0) in the XRD patterns and these are characteristic to the layer structure. In this work, the intensity ratio I(003)/I(104) of $Li_{1.10}Ni_{0.30}Co_{0.30}Mn_{0.40}O_2$ material was 1.30. Since the intensity ratio I(003)/I(104) was sensitive to the cation ordering in the lattice, excellent electrochemical activity can be expected for this material. The intensity ratio I(003)/I(104) was high and two double peaks of (006)/(102) and (108)/(110) were split clearly, indicating that the sample was well-crystallized with ordered, layered structure. The electrochemical performance of the battery depends directly on the particle size, particle size distribution and the morphology of the cathode materials as well. Materials with a smaller particle size tend to have high capacity, and uniform particle size distribution leads to enhance overall battery performance by the uniform depth of charge of each particle. The SEM image of the $Li_{1.10}Ni_{1/3}Co_{1/3}Mn_{1/3}O_2$ is shown in Fig. 2. It indicates that the material synthesized by the sol–gel method showed non-agglomerated nanosized particles. It showed that the original particles are of the size range of 300 – 400 nm with good shape.

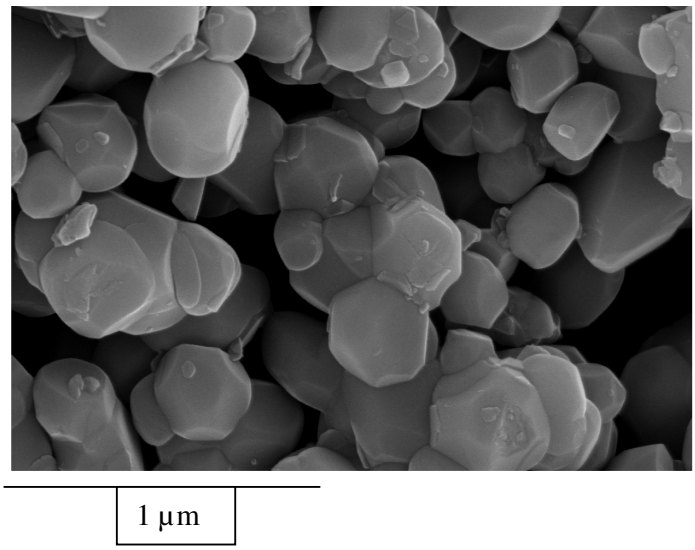


**Figure 2.** SEM of $Li_{1.10}Ni_{1/3}Co_{1/3}Mn_{1/3}O_2$ material prepared by sol-gel process sintered at 850°C

Fig. 3 reports the charge and discharge curves for the first cycle of the $LiNi_{1/3}Co_{1/3}Mn_{1/3}O_2$ and $Li_{1.10}Ni_{1/3}Co_{1/3}Mn_{1/3}O_2$ electrodes, for which the cycling was carried out at a constant current rate of 0.1C between potential limits of 2.5 V and 4.3 V. The first discharge capacity of the $Li_{1.10}Ni_{1/3}Co_{1/3}Mn_{1/3}O_2$ electrode is some 10 mAh/g higher than that of $LiNi_{1/3}Co_{1/3}Mn_{1/3}O_2$ electrode. In addition, the irreversible capacity loss of the $Li_{1.10}Ni_{1/3}Co_{1/3}Mn_{1/3}O_2$ electrode is relatively lower (3 %) when compared to that of $LiNi_{1/3}Co_{1/3}Mn_{1/3}O_2$ electrode (7 %). In order to evaluate the effect of excess lithium on the rate capability of $LiNi_{1/3}Co_{1/3}Mn_{1/3}O_2$, the cells were initially cycled in the voltage range 2.5–4.3 V. Fig. 4a & b shows the discharge curves of $LiNi_{1/3}Co_{1/3}Mn_{1/3}O_2$, $Li_{1.10}Ni_{1/3}Co_{1/3}Mn_{1/3}O_2$ and cells cycled at various current rates between voltage limits of 2.5 and 4.3 V, respectively. The cell was charged using a current rate of 0.1 C before each discharge testing.

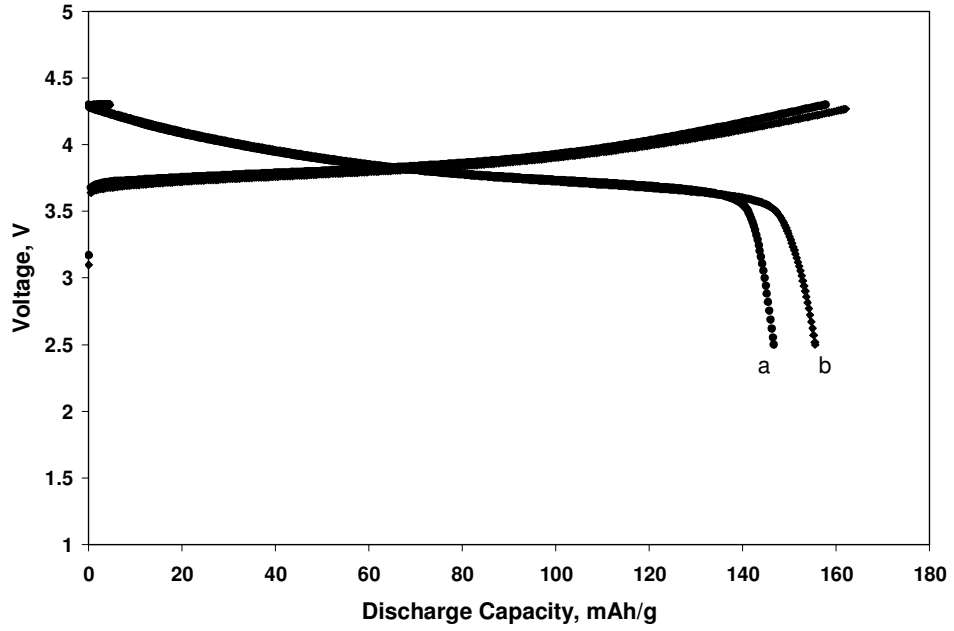


**Figure 3.** Initial charge and discharge curves of (a) $LiNi_{1/3}Co_{1/3}Mn_{1/3}O_2$ and (b) $Li_{1.10}Ni_{1/3}Co_{1/3}Mn_{1/3}O_2$coin-cells in the voltage range 2.5 - 4.3V at 0.1C.

Rate capability test shows interesting results. Fig. 4 shows the discharge capacities of the $LiNi_{1/3}Co_{1/3}Mn_{1/3}O_2$ and Li-rich $Li_{1.10}Ni_{1/3}Co_{1/3}Mn_{1/3}O_2$ cells as a function of C rate between 3.0 and 4.5 V vs Li. The cells were charged galvanostatically with a 0.1 C rate before each discharge testing, and then discharged at different C rates from 0.1 to 8 C rates (16–1280 mA/ g). Clearly, the Li-rich $Li_{1.10}Ni_{1/3}Co_{1/3}Mn_{1/3}O_2$ delivered a higher discharge capacity than the $LiNi_{1/3}Co_{1/3}Mn_{1/3}O_2$, at all the tested C rates. Although the $LiNi_{1/3}Co_{1/3}Mn_{1/3}O_2$ showed an abrupt discharge capacity at higher C-rate, the Li-rich $Li_{1.10}Ni_{1/3}Co_{1/3}Mn_{1/3}O_2$ electrode retained its higher discharge capacity. At 8C rate, the obtained discharge capacity of the Li-rich $Li_{1.10}Ni_{1/3}Co_{1/3}Mn_{1/3}O_2$ was about 79%, compared to that of a 0.1 C rate, while the $LiNi_{1/3}Co_{1/3}Mn_{1/3}O_2$ electrode showed capacity retention of only 74% at the same C rate. This result clearly shows the excess Li impact on the electrochemical performance.

Cycleability test illustrates more interesting results. The cycling performance of the $Li_{1.10}Ni_{1/3}Co_{1/3}Mn_{1/3}O_2$ and $LiNi_{1/3}Co_{1/3}Mn_{1/3}O_2$ electrodes were measured at a current of 8C between 2.5 and 4.3 V. Fig. 5 indicates that the cycling performance of Li-rich and stoichiometric $LiNi_{1/3}Co_{1/3}Mn_{1/3}O_2$ electrode materials cycled at a high current rate of 8C. After 30 charge-discharge cycles, the $Li_{1.10}Ni_{1/3}Co_{1/3}Mn_{1/3}O_2$ electrode exhibits excellent cycling performance with capacity retention ratio of about 91% when compared to that of $LiNi_{1/3}Co_{1/3}Mn_{1/3}O_2$ electrode which shows only 80% capacity retention ratio. The improved electrochemical performance of Li-rich $LiNi_{1/3}Co_{1/3}Mn_{1/3}O_2$ electrode material could be due to the formation of two components like $xLi_2MnO_3$. $(1-x)LiMO_2$ (M=Ni, Co, Mn) in which two layered compounds are structurally integrated to form highly complex atomic arrangements [26]. The $Li_2MnO_3$ component available in the transition

metal layer imparts quite interesting electrochemical performance in the electrode materials. Since the manganese ions of the $Li_2MnO_3$ are structurally connected to the $LiMO_2$ and participate in the electrochemical reaction, the electrode delivers high reversible capacity even at high C-rate as can be seen in Fig. 5. The excess lithium resides in the transition metal layer forms $Li_2MnO_3$ like domains by cation ordering with manganese ions. Therefore, the excess lithium in $Li_{1.10}Ni_{1/3}Co_{1/3}Mn_{1/3}O_2$ is expected to influence the electronic and crystallographic structure by forming a composite material like $xLi_2MnO_3$. $(1-x)LiMO_2$ (M=Ni, Co, Mn). This results an enhancement in the electrochemical performance of the materials by excess lithium content. Significantly improved rate capability and cycleability (at high C-rate) of the Li-rich $Li_{1.10}Ni_{1/3}Co_{1/3}Mn_{1/3}O_2$ electrode synthesized in this work clearly demonstrates its advantage for use in high power lithium ion batteries.

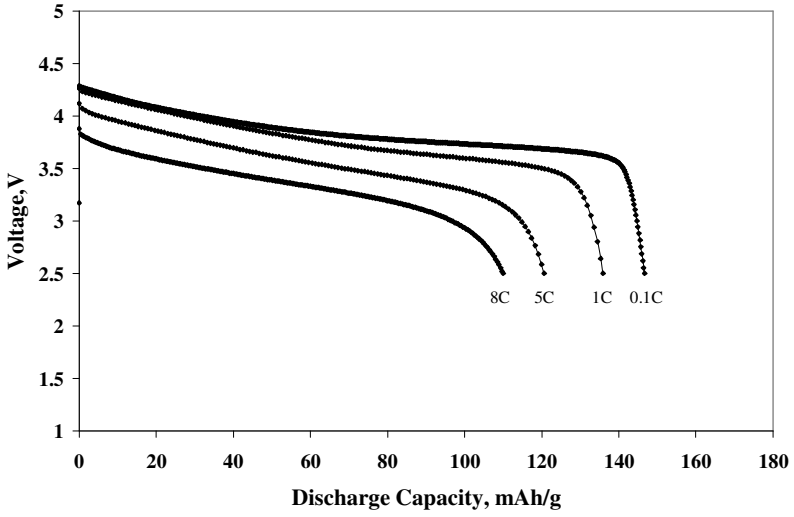


(a)

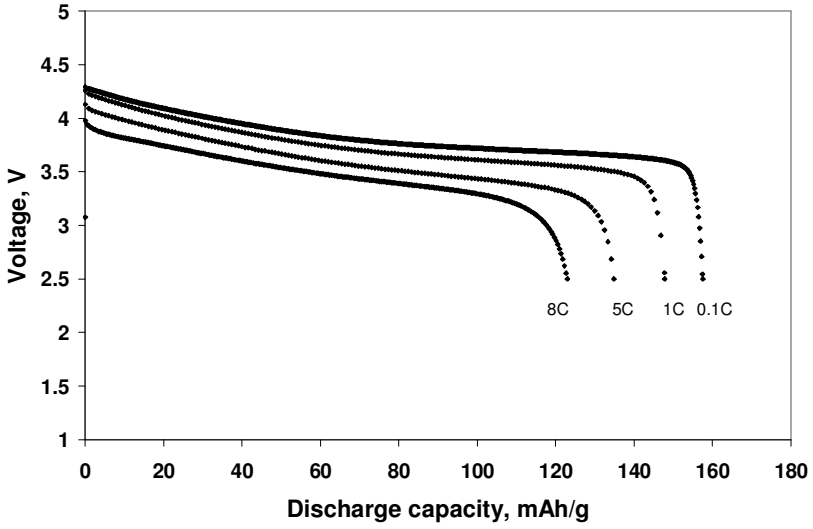


(b)

**Figure 4.** Discharge curves of (a) $LiNi_{1/3}Co_{1/3}Mn_{1/3}O_2$and (b) $Li_{1.10}Ni_{1/3}Co_{1/3}Mn_{1/3}O_2$ coin-cells in the voltage range 2.5 - 4.3V at various current rates 0.1 to 8C.

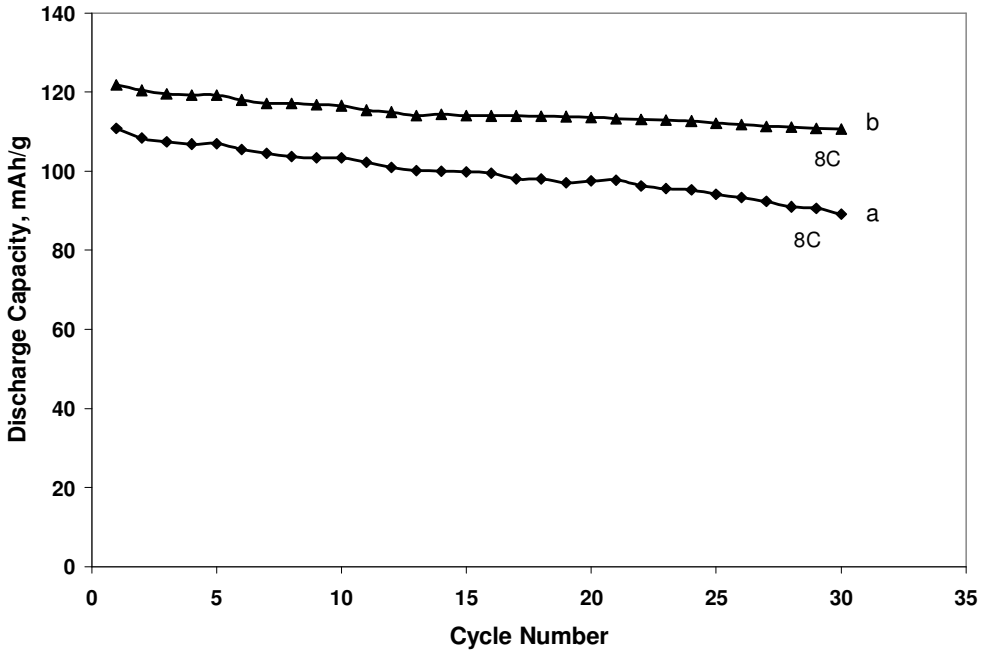


**Figure 5.** Discharge capacity Vs Cycle number plots of (a) $LiNi_{1/3}Co_{1/3}Mn_{1/3}O_2$ and (b) $Li_{1.10}Ni_{1/3}Co_{1/3}Mn_{1/3}O_2$ coin-cells in the voltage range 2.5 - 4.3V at 8C

## 4. CONCLUSIONS

Well-ordered layered Li-rich $Li_{1.10}Ni_{1/3}Co_{1/3}Mn_{1/3}O_2$ cathode material was successfully prepared by sol-gel process and characterized for its structural, morphological and electrochemical properties. The Li-rich $Li_{1.10}Ni_{1/3}Co_{1/3}Mn_{1/3}O_2$ showed much improved rate capability and cycling stability compared to stoichiometric $LiNi_{1/3}Co_{1/3}Mn_{1/3}O_2$. The Li-rich material showed only 9% capacity loss after 30 cycles at a high C-rate of 8C in the voltage range between 2.5V and 4.3V while the stoichiometric material suffered 20% capacity loss. Such excellent properties could have originated from the more stabilized structure of Li-rich materials when compared to that of stoichiometric material. The improved structural stability could be related to formation of $Li_2MnO_3$ by excess lithium available in the transition metal layer.

ACKNOWLEGEMENTS

This work is supported by U.S-DOD-ARO-Electrochemistry and Advanced Energy Conversion Division under the grant # W911NF-08-C-0415 (Proposal No: 52322-CH-H (BOBBA)). BRB and R. Santhanam thank Dr. Robert Mantz for supporting cathode materials research for developing hybrid energy storage devices.

## References

1. P. G. Bruce, B. Scrosati, J. M. Tarascon, *Angew. Chem. Int. Ed*. 47 (2008) 2.

2. M. S. Whittingam, *Chem. Rev*. 104 (2004) 4271.
3. J. M. Tarascon, M. Armond, *Nature* 414 (2001) 359.
4. J. S. Bok, J. H. Lee, B. K. Lee, *Solid State Ionics* 169 (2004) 139
5. J. Ying, C. Jiang, C. Wan, *J. Power Sources*, 129 (2004) 264
6. T. Ohzuku and Y. Makimura, *Chem. Lett*., 2001, 642.
7. T. Ohzuku and Y. Makimura, *Chem. Lett*., 2001, 744.
8. S. Patoux, M. M. Doeff, *Electrochem. Commun*. 6 (2004) 767.
9. Z. Lu, D. D. MacNeil, J. R. Dahn, *Electrochem. Solid State Lett*. 4 (2001) A191.
10. B. J. Hwang, Y. W. Tsai, D. Carlier, G. Ceder, *Chem. Mater*. 15 (2003) 3676.
11. Y. K. Sun, S. W. Cho, S. W. Lee, C. S. Yoon, K. Amine, *J. Electrochem. Soc*. 154 (2007) 168.
12. S. B. Schouguard, J. Breger, M. Jiang, C. P. Grey, J. B. Goodenough, *Adv. Mater.* 18 (2006) 905.
13. J. Choi, A. Manthiram, *J. Electrochem. Soc*. 152 (2005) 1714.
14. K. Kang, Y. S. Meng, J. Breger, C. P. Grey and G. Ceder, *Science*, 311 (2006) 977.
15. B. J. Hwang, T. H. Yu, M. Y. Cheng, R. Santhanam, *J. Mater. Chem.* 19 (2009) 4576.
16. W. Yoon, C.P. Grey, M. Balasubramanian, X.Q. Yang, D.A. Fisher, J. McBreen, *Electrochem. Solid-State Lett*. 7 (2004) A53.
17. W. Yoon, C.P. Grey, M. Balasubramanian, X.Q. Yang, Z. Fu, D.A. Fisher, J. McBreen, *J. Electrochem. Soc*. 151 (2004) A246.
18. G.H. Kim, S.T. Myung, H.J. Bang, J. Prakash, Y.K. Sun, *Electrochem. Solid-State Lett*. 7 (12) (2004) A477.
19. S.K. Kim, W.T. Jeong, H.K. Lee, J. Shim, *Int. J. Electrochem. Sci.* 3 (2008) 1504.
20. P. Periasamy, N. Kalaiselvi, H.S. Kim, *Int. J. Electrochem. Sci.* 2 (2007) 689.
21. S. H. Park, H. S. Shin, S. T. Myung, C. S. Yoon, K. Amine, Y. K. Sun, *Chem. Mater*. 17 (2005) 6.
22. S. Patoux, M. M. Doeff, *Electrochem. Commun*. 6 (2004) 767.
23. Y. Fujii, H. Miura, N. Suzuki, T. Shoji, N. Nakayama, *J. Power Sources*, 171 (2007) 894.
24. X. Luo, X. Wang, L. Liao, S. Gamboa, P. J. Sebastian, *J. Power Sources*, 158 (2006) 654.
25. S. K. Hu, G. H. Cheng, M. Y. Cheng, B. J. Hwang, R. Santhanam, *J. Power Sources*, 188 (2009) 564.
26. M. M. Thackeray, C. S. Johnson, J. T. Vaughey, N. Li, S. A. Hackney, *J. Mat. Chem*. 15 (2005) 2257.
27. B. J. Hwang, R. Santhanam, D. G. Liu, *J. Power Sources*, 97-98 (2001) 443.
28. Z. Chen, J.R. Dahn, *Electrochem. Solid-State Lett*. 5 (2002) A213.
29. T. Ohzuku, A. Ueda, M. Nagayama, Y. Ieakoshi, H. Komori, *Electrochim. Acta* 38 (1993) 1159
30. Y. Gao, M.V. Yakovleva,W.B. Ebner, *Electrochem. Solid-State Lett*. 1 (1998) 117.